EFFECT OF FLUX PENETRATION ON THE LOAD CAPACITY OF PASSIVE SUPERCONDUCTING BEARINGS

DANTAM K. RAO
Mechanical Technology Inc.
968 Albany-Shaker Road
Latham, NY, 12110

ABSTRACT

The past year has seen a dramatic improvement in the load capacity of a superconductor-magnet pair. The measured load capacities that stood at 0.1 psi two years back have been improved now to an impressive 40 psi. This improvement is mainly due to better processing techniques developed by the superconducting material processing community. Our analysis indicates that, by using these processing techniques that efficiently prevent flux penetration, we can achieve high load capacities. With these developments, it is possible to insert passive bearings into actual applications within the next few years time frame.

1. INTRODUCTION

Passive Superconducting Bearings (PSB) differ from active magnetic bearings in that they use bulk superconductors to stably levitate a body without using complex control systems and without expenditure of external power (Rao and Dill [1]). A magnet-superconductor pair, consisting of a permanent magnet (PM) and a high temperature superconductor (HTS), separated by a magnetic gap, as shown in Figure 1, forms a typical stable bearing. The static load capacity (commonly called "load capacity") of such a pair is defined as the contact force exerted by the superconductor divided by the load bearing area of the suspended magnet. In the USA, the force is expressed in pounds while the load bearing area is expressed as square inches, so that the units are pounds per square inch or psi.

About two years back, the load capacity of this arrangement, measured at 77K, stood at 0.1 psi. Now, thanks to the immense efforts by the superconducting material development community, improved material processes are available, and the load capacities as high as 40 psi (a 400 -fold increase) can be obtained per Rao [2] and Murakami et al [3]. At lower temperatures of 4 K, recent tests indicate that we can achieve up to 100 psi using these materials per Moon.* It is known that the flux penetrates the superconductor partially, and thus degrades the load capacity. Even though considerable effort has been made in predicting the levitation forces, the force generation mechanism is not fully understood (see Moon [4] for a review of force models) when the gaps are small. An improved understanding of the force generation mechanism at small gaps is currently needed, and this forms the subject matter of this paper.

2. LEVITATION FORCE

2.1 General formula for force

As shown in Figure 2, let (r,θ, z) denote the cylindrical coordinate system erected at the center of the active surface of the superconductor. At a point $P(r,\theta, z)$ inside the superconductor, let $\mathbf{B_m}(P)$ [tesla or N/Am] denote the flux density applied by the magnet alone in free space. As we bring the magnet closer to the superconductor, its moving flux lines cut "rings" of superconductor

*Moon, F., Private Communication, 1991.

material and induce currents of density $\mathbf{J_s}$ [A/m^2] in them. The net field **B** at the point P is $\mathbf{B_m}$ plus the self field $\mathbf{B_i}$ (i.e, the field created by all induced currents) so that $\mathbf{B} = \mathbf{B_m} + \mathbf{B_i}$. The induced currents **Js** interact with this net field **B** to create a net body force $\mathbf{J_s} \times \mathbf{B} = \mathbf{J_s} \times \mathbf{B_m} + \mathbf{J_s} \times \mathbf{B_i}$. But since the force components due to self-field (i.e., $\mathbf{J_s} \times \mathbf{B_i}$) are internal, they cancel each other, leaving a body force $\mathbf{J_s} \times \mathbf{B_m}$ external to the superconductor. Thus the force equals the superconductor's current density $\mathbf{J_s}(P)$ times magnet's field $\mathbf{B_m}$ (P) integrated over the volume V of the superconductor, viz.

$$F = \int_V J \times B_m \, dv \tag{1}$$

2.2 Superconductor

Macroscopically, we model the superconductor as a collection of closed loop "ring elements", each of which can carry persistent currents of density $\mathbf{J_s}(P)$ as discussed above. The general form for the superconductor's magnetization vector is $\mathbf{M_s} = M_r\,\mathbf{r} + M\theta\,\theta + M_z\,\mathbf{z}$. Because of axisymmetry, however, the tangential component vanishes [$M\theta = 0$] so that $\mathbf{M_s}$ simplifies to $\mathbf{M_s} = M_r\,\mathbf{r} + M_z\,\mathbf{z}$, where the components Mr, Mz depend only on r,z coordinates. We substitute this in the Maxwell's law $\mathbf{J_s} = \nabla \times \mathbf{M_s}$ to compute current density by (2). Note that as a first approximation, we may estimate the magnetization components M_r, M_z from the measured magnetization curve $M(B_m(P))$ and use them to compute $\mathbf{J_s}$ from (2). Equation (2) shows that the current density $\mathbf{J_s}$ at a point P is the difference between the axial gradient of the radial component of magnetization and the radial gradient of the axial component of magnetization, both evaluated at that point P.

$$J_s = J_\theta\,\hat{\theta} = \left(\frac{\partial M_r}{\partial z} - \frac{\partial M_z}{\partial r} \right) \hat{\theta} \tag{2}$$

2.3 Magnet

The general form for magnet's field is $\mathbf{B_m} = B_r\ \mathbf{r} + B\theta\ \theta + B_z\ \mathbf{z}$. We also assume that the magnet's field is axisymmetric. The axisymmetry implies that tangential component vanishes ($B\theta = 0$) and the radial and axial components B_r and B_z depend only on r and z. This reduces the magnet's field $\mathbf{B_m}$ to

$$B_m = B_r\ \hat{r} + B_z\ \hat{z} \tag{3}$$

2.4 Magnet-superconductor Interaction Force

Substituting (2) and (3) in (1) indicates that the interaction force has only the levitation (i.e., axial) component F_z, which is given by

$$F = F_z\ \hat{z} \tag{4}$$

$$F_z = -\int J_\theta\ B_r\ dv \tag{5a}$$

$$= \int_V \left(\frac{\partial M_z}{\partial r} - \frac{\partial M_r}{\partial z} \right) B_r\ dV \tag{5b}$$

Thus levitation force F_z is the product of the current density $J\theta$ in the superconductor and the magnet's radial field component B_r, integrated over the

entire volume of the superconductor. The radial component of force turns out to be zero, which is consistent with the axisymmetry of the pair.

3. FINITE ELEMENT FIELD CALCULATION RESULTS

In this section, we examine the distribution of the applied field B_r along the radial (and axial) directions. We believe that this spatial nonuniformity of fields greatly affects the estimate of the repulsive force. The levitation force also varies with many other parameters [2], but we have not focussed on these other effects herein. In order to understand the field distribution, we used a finite element code called MAXWELL [5] to plot the flux lines. We used a small magnetic gap of 0.020 in (015 mm) in our calculations.

Figure 3 shows the mesh elements used to model the space occupied by the magnet and superconductor. We found that, in order to achieve a fair degree of accuracy, the regions around the magnetic gap must be represented by meshes that are finer than those in other regions. We used 7676 elements.

Figure 4 shows how the superconductor affects the flux lines from a magnet. For the magnet in free space, the flux lines emanate from it axially but become nearly radial by the time they reach its edge (i.e., they bend by 90 degrees). With the insertion of the superconductor, these flux lines are literally compressed and squeezed inside the narrow magnetic gaps. This flux line compression causes the radial field to be highest around the edge of the magnet and hence increases net force.

Figure 5 compares the experimental and theoretical distribution of flux density applied by the magnet in the axial direction. The experimental and theoretical results are in good agreement, showing that we can simulate the fields with confidence.

In Figure 6 we show how the radial flux density varies with the radial position. It shows that the effect of the superconductor is to nearly double the radial flux density at the periphery of the magnet, from 0.4 tesla to 0.8 tesla (if the

superconductor does not allow any flux penetration). This field increases up to the magnet's diameter and then falls down beyond it.

This general trend in field distribution is confirmed by the calculations done by Argonne National Laboratory recently [6] as shown in Figure 7. The curve (a), plotted by MTI, corresponds to a 20mm diameter magnet while the curve (b) plotted by ANL, corresponds to a 3.2 mm diameter PM [6].

From this plot we conclude that: (1) the radial component of the applied field starts as zero at the center, (2) it increases to a maximum value at the edge of the magnet and then (3) it decreases to a near-zero value at the edge of the superconductor.

4. EXPERIMENTAL AND ANALYTICAL INVESTIGATIONS OF REPULSIVE FORCE

As a first step towards analysis, we measured the force of repulsion between a permanent magnet and a superconductor using a specially designed levitation test rig. We then calculated the force of repulsion using the MAXWELL finite element program to solve the Maxwell equations. Figures 8 through 10 display the results of these experimental and analytical investigations.

Figure 8 shows the measured variation of repulsive force with the magnetic gap. The operational gap range for bearings is usually less than 0.1 in. (2.5 mm). In this range, this plot shows that the force increases in an almost straight line fashion with the magnetic gap. This linearity of force with gap greatly simplifies the analysis and design of passive bearing elements. It is fair to add that this linearity depends on the process of the material.

Figure 9 shows how the computed force of repulsion is influenced by the flux penetration. A magnetic gap of 0.020 in. has been used in these calculations. When the superconductor is diamagnetic (i.e., has a near-zero relative permeability), Figure 9a shows that it does not allow any flux to penetrate, and the force of repulsion is extremely high, of the order of 16 lb. At a relative

permeability of 0.1, the flux begins to penetrate, and we observe degradation of the load capacity to 13 lb. As the relative permeability increases to 0.4, Figure 9d shows a repulsive force of 7.6 lb; this value is quite close to the measured data.

As already indicated, only gaps in the range of up to 0.1 in. is of interest to the bearing designer. Hence we replotted in Figure 10 the experimental and analytical results in this range of interest. This figure shows that there is a good degree of correlation between the experimental and analytical force-gap data. It shows that we can predict (in the small gap range that is of interest to the bearing designer) the repulsion force between the magnet and superconductor with a fair degree of accuracy.

5. SUMMARY

In this paper we have indicated that the superconductor material technology has greatly improved over the past two years to the extent that load capacities of up to 40 psi can be achieved at 77 K temperature with the currently available materials. These load capacities are sufficiently high so that we can construct and test the passive bearings within the next few years. We can also predict and analyze the bearing forces with confidence in the small gap ranges of interest to the bearing designer (i.e., 0 to 0.1 in.).

REFERENCES

[1] Rao, D.K., and Dill, J.F., "Comparative Assessment of Single Axis Force Generation Mechanism for Superconducting Suspensions", Proc. 25th IECEC, Vol. 5, pp. 149-153, 1990.

[2] Rao, D.K., "Load Capacity of Passive Superconducting Levitation Systems", presented in the Magnetic Bearings and Dry Gas Seals Conference, Mar. 13-15, 1991, Washington D.C.

[3] Murakami, H. et al., "Large Levitation Force due to Flux Pinning of MPMG Processed YBCO Superconductors with Ag Doping,", Proc. ISS, 1991.

[4] Moon, F.C., "Magnetic Forces in High-Tc Superconducting Bearings", Applied Electromagnetic in Materials, Vol. 1, 1990, pp. 29-35.

[5] MAXWELL - User's Manual. 1991.

[6] Cha, Y.S., Hull, J.R., Mulcahy, T.M., and Rossing, T.D.,"Effect of size and Geometry of Levitation Force Measurements between Permanent Magnets and High-Temperature Superconductors", Proc. 5th Joint MMM Intermag. Conference, Pittsburgh, PA, June 18-21, 1991.

[7] Chang, P.-Z.,"Mechanics of Superconducting Magnetic Bearings", Ph.D Thesis, Cornell University, Jan. 1991.

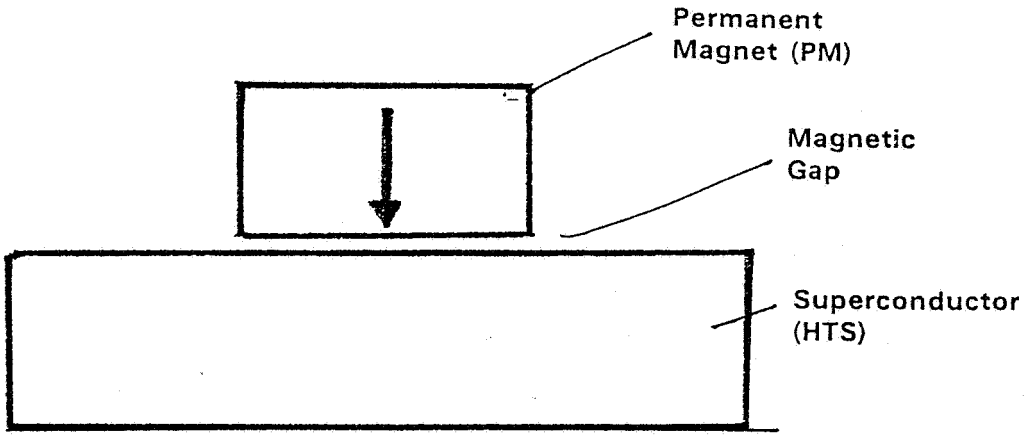

Figure 1. Typical magnet-superconductor pair producing stable levitation.

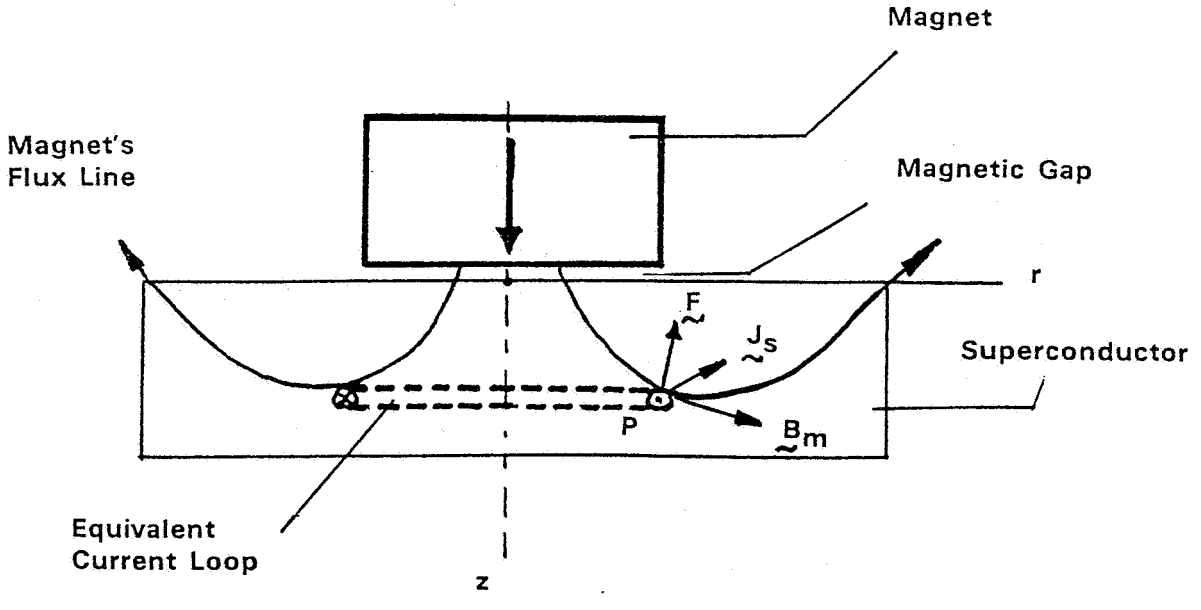

Figure 2. A magnet with flux density B_m interacts with a "ring element" with current density J_S to create a Lorentz force $J_S \times B_m$.

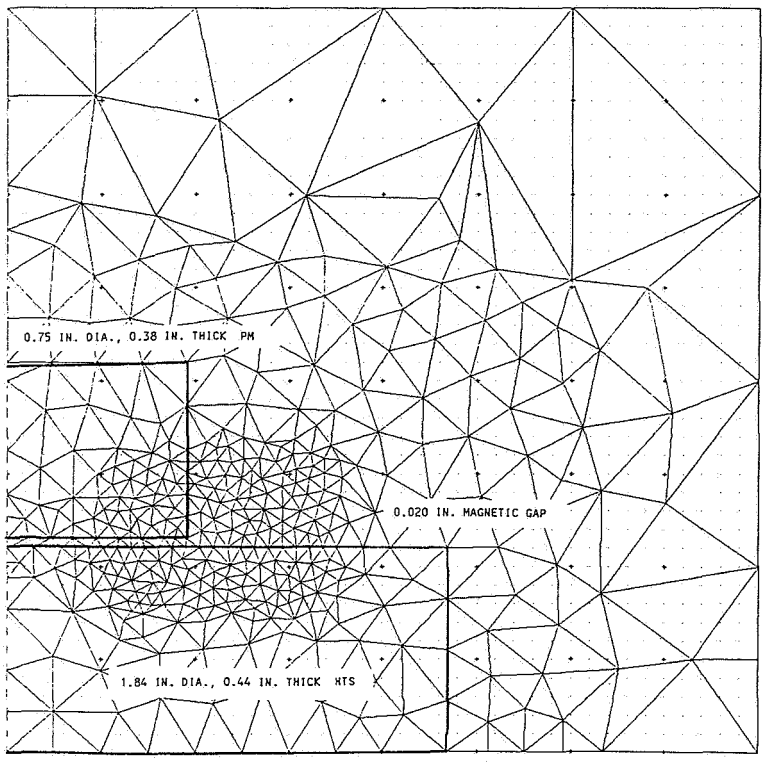

Figure 3. Finite element mesh used to generate flux line plots of magnet-superconductor.

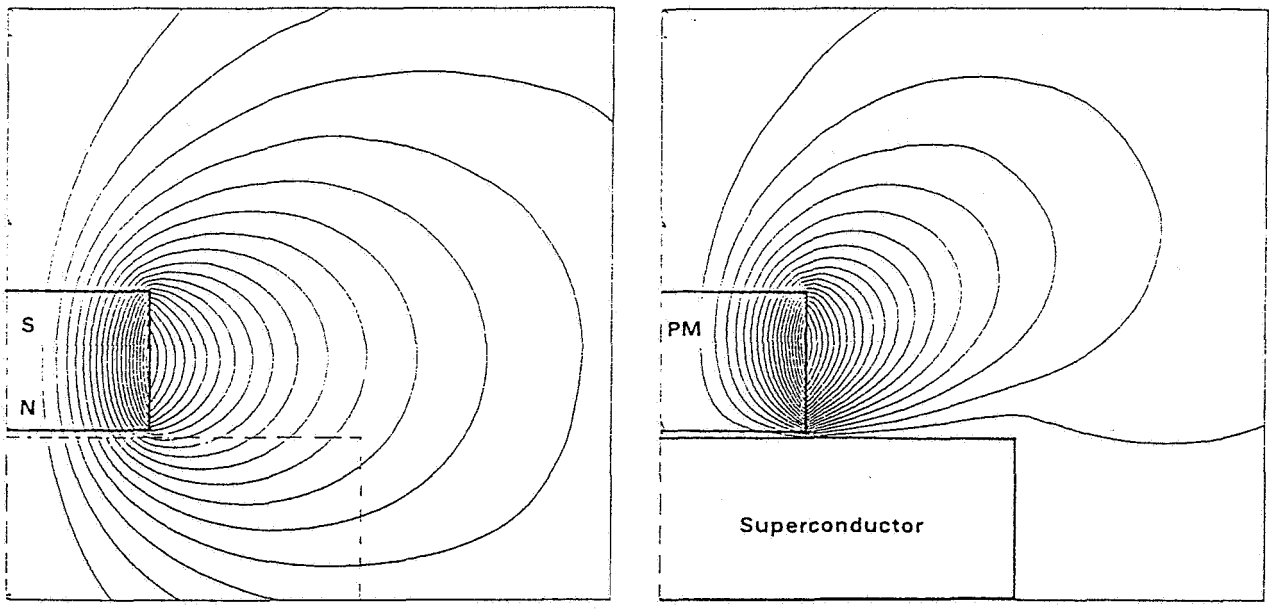

Figure 4. Flux line plots — (a) magnet alone and (b) with the superconductor.

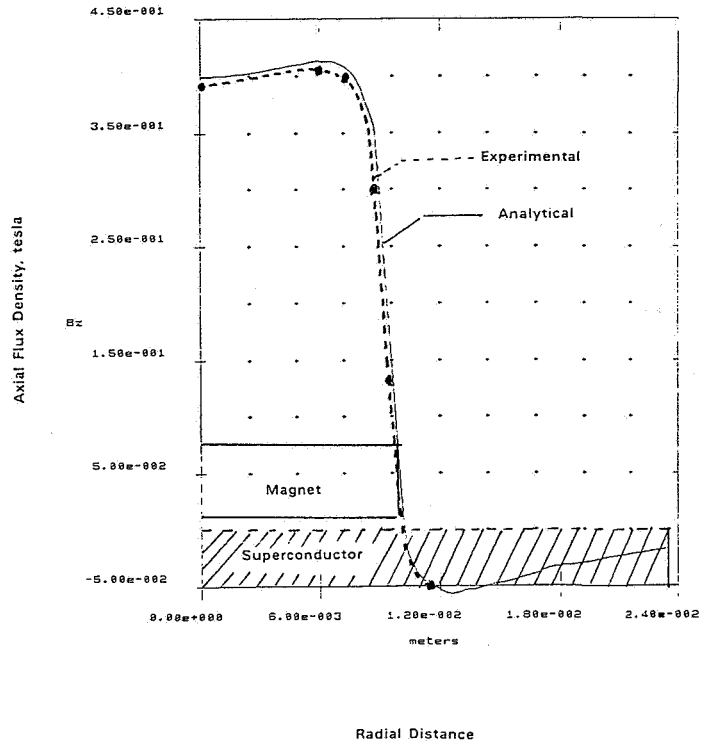

Figure 5. Spatial distribution of flux density along the axial direction. (a) analytical, (b) experimental.

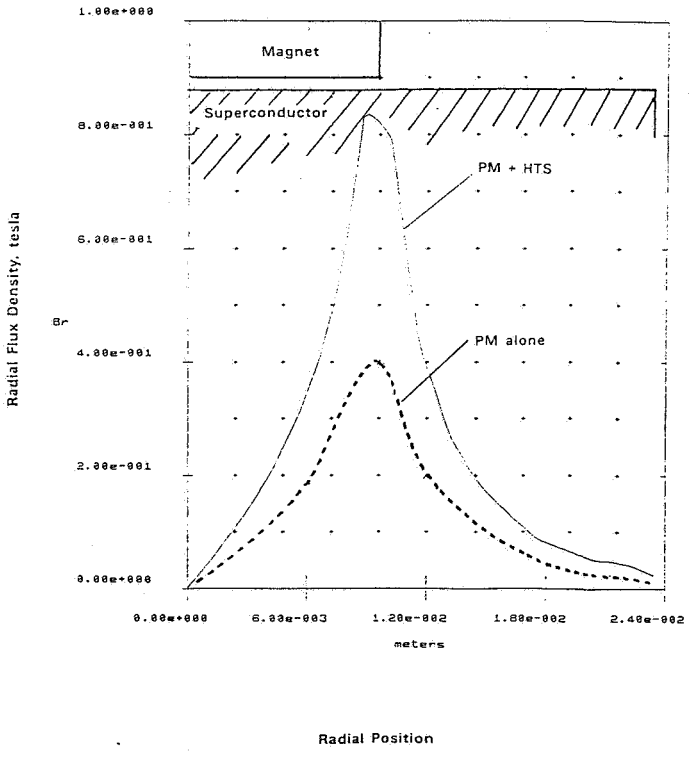

Figure 6. Variation of the field applied a magnet with and without the superconductor.

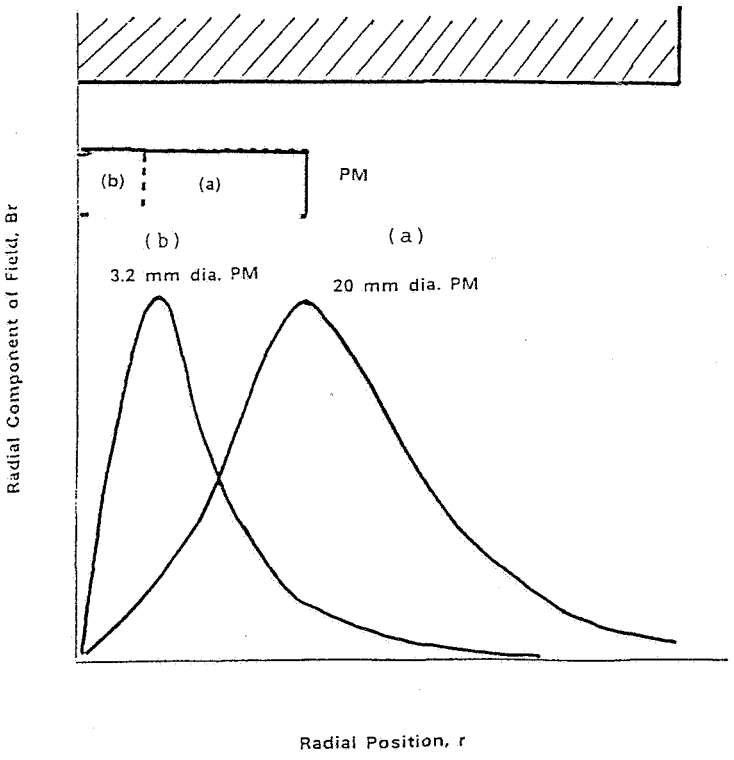

Figure 7. Comparison of fields applied by magnets of different sizes on the superconductor.

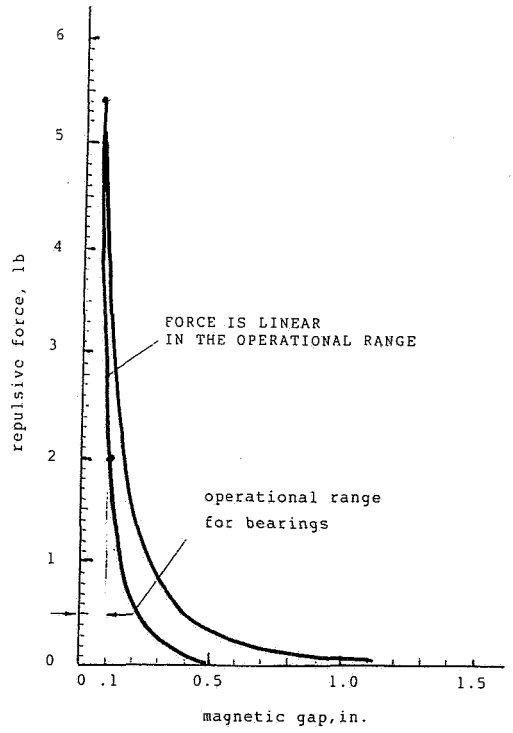

Figure 8. Repulsion force measured between a permanent magnet and a superconductor.

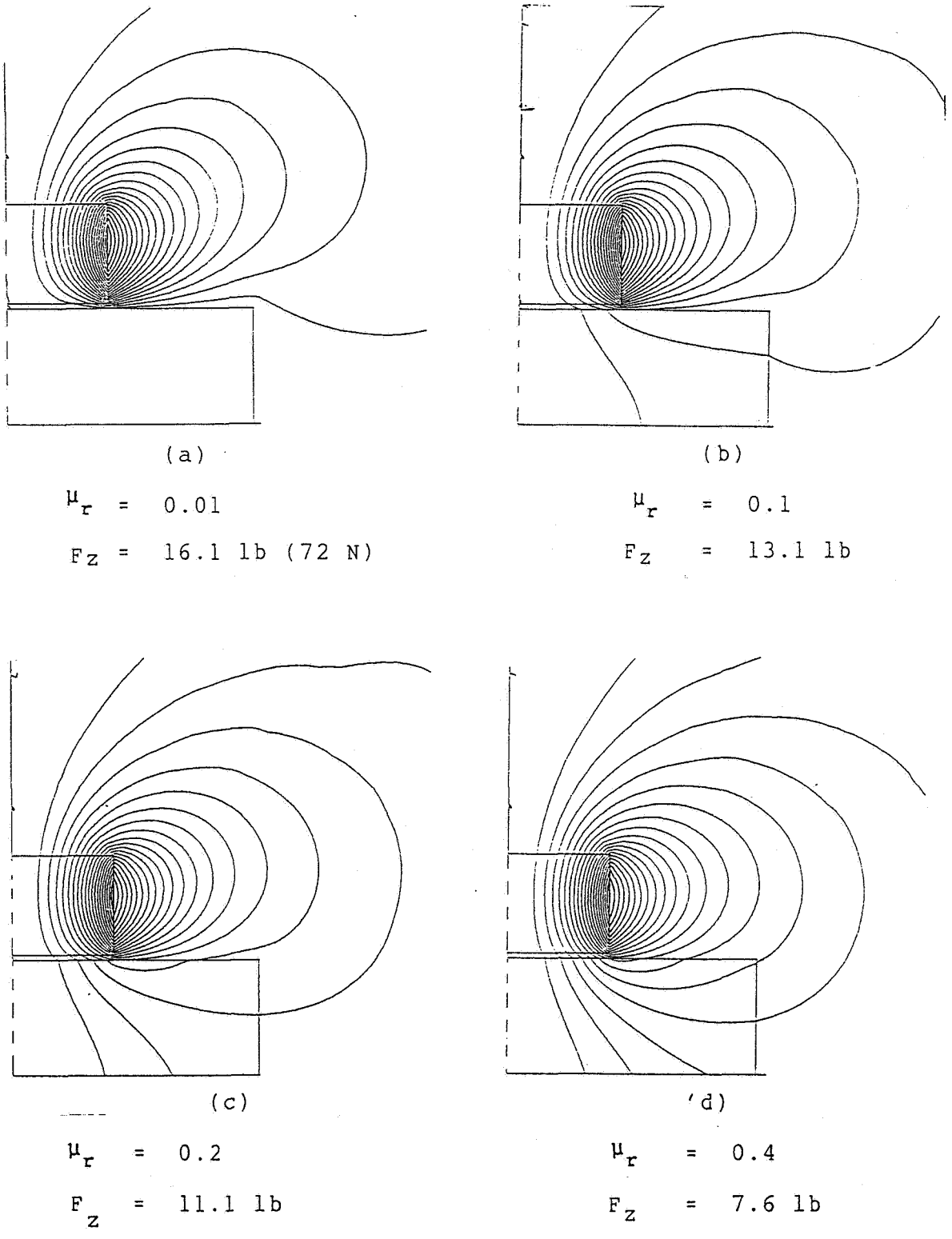

Figure 9. Effect of penetration of flux on the load capacity of a magnet-superconductor pair.

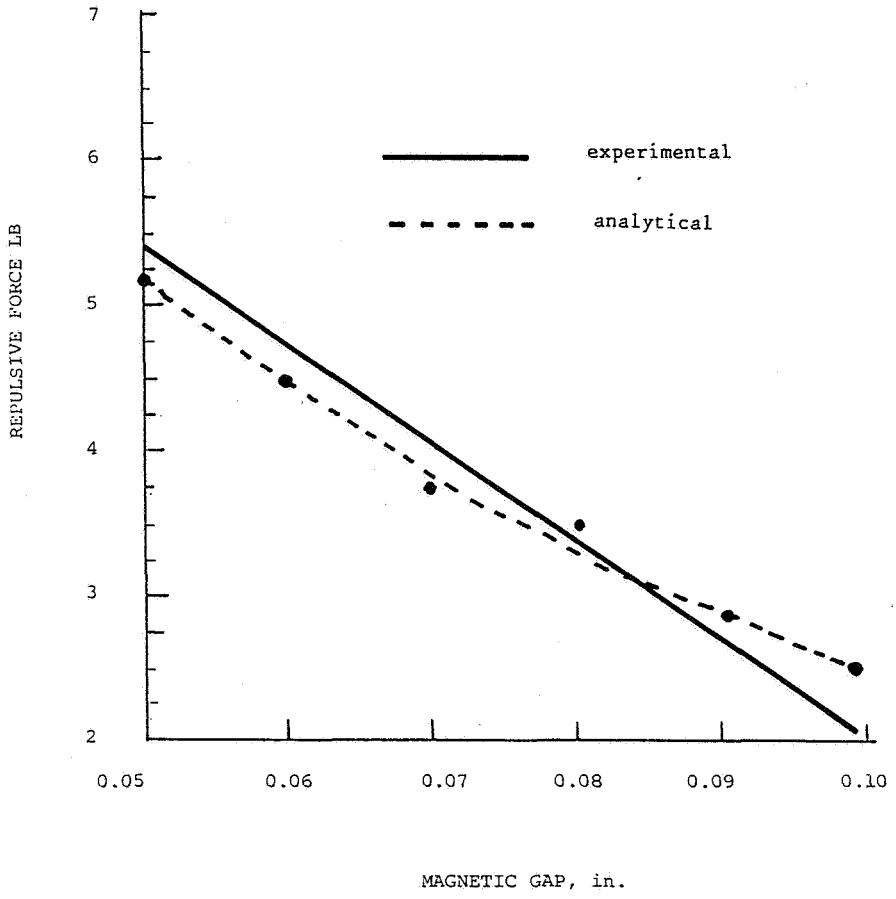

Figure 10. Comparison of analytical and experimental results of repulsive force at small gaps.